Colloids and Surfaces A: Physicochem. Eng. Aspects 426 (2013) 1–5

Contents lists available at SciVerse ScienceDirect

Colloids and Surfaces A: Physicochemical and Engineering Aspects

journal homepage: www.elsevier.com/locate/colsurfa

Interfacial tension between oil and water measured with a modified contour method

F. Peters*, D. Arabali

Strömungsmechanik, Ruhr-Universität Bochum, D-44780 Bochum, Germany

HIGHLIGHTS

- An experimental method is presented for the interfacial tension between two liquids.
- The bubble contour is evaluated by image processing.
- A force balance is used for the interfacial tension.
- The Laplace equation relating internal pressure and curvature is not involved.

GRAPHICAL ABSTRACT

The interfacial tension between silicon oil (AK20) and water measured by a novel contour method not using the Laplace equation.

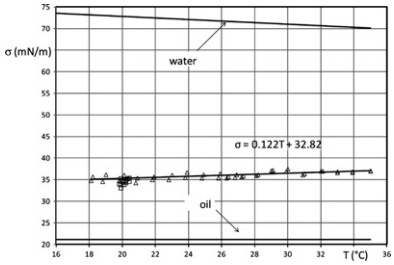

ARTICLE INFO

Article history:
Received 19 November 2012
Received in revised form 28 February 2013
Accepted 6 March 2013
Available online 13 March 2013

Keywords:
Interfacial tension measurement
Pendant drop
Image processing
Oil/water system

ABSTRACT

The interfacial tension between silicone oil and water is measured in the temperature range 18–35 °C. A novel method is used which promises prospects for the application to other liquid/liquid systems. The method is based on digital image processing of the contour of a pendant drop in combination with a pressure measurement. In contrast to existing algorithms axisymmetric drop shape analysis (ADSA) relying on iterative solutions of the Laplace equation the interfacial tension is obtained without Laplace from a force balance yielding an explicit expression for the interfacial tension.

1. Introduction

The classical methods of surface tension measurement like the ring or the capillary tube method have been around for decades and some of them are insurmountable with respect to simplicity and expenses. For a full account see, e.g. Adamson and Gast [1]. Nevertheless, with the advent of image processing the Laplace-contour methods have gained ground and found their way into commercial instruments. They are based on the Laplace equation which relates the pressure jump across the surface to the surface tension and the local curvature in two Cartesian directions. The measurement of the local 2-D curvature at the required high level of accuracy is extremely difficult. Therefore, the common approach reduces the problem to symmetry with respect to the drop (or bubble) axis supposing that all axial–radial cross sections are identical. Then one of the two curvatures comes from a measurable diameter and the other reduces to a digital contour surveying. This is the case with pendant or sessile drops or bubbles. A current name for these methods is axisymmetric drop shape analysis (ADSA). A comprehensive review is found in Ref. [2] providing much of the long history of ADSA. The state of the art is given by Alvarez et al. [3] who point to the mathematical difficulties with ADSA occurring at small Bond numbers, i.e. towards spherical bubbles.

* Corresponding author. Tel.: +49 2343226429.
E-mail address: franz.peters@rub.de (F. Peters).

0927-7757/$ – see front matter © 2013 Elsevier B.V. All rights reserved.
http://dx.doi.org/10.1016/j.colsurfa.2013.03.010

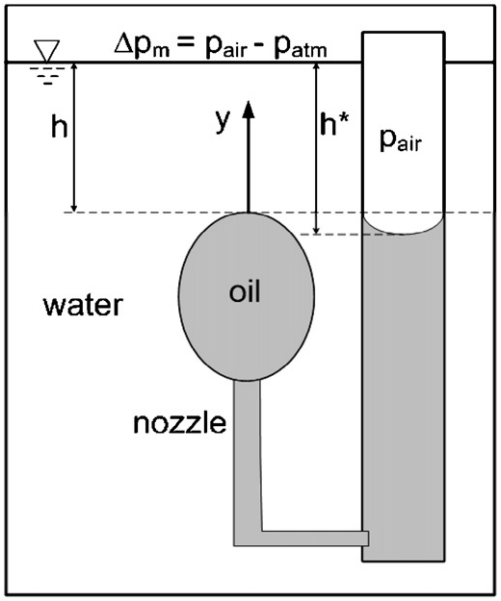

Fig. 1. Principle arrangement of oil bubble in water.

ADSA is mathematically challenging and elegant. Yet, it must not be overlooked that it is bound to the quality of the experimental contour data. Even if the bubble is perfectly symmetric digital imaging has its limits due to pixel resolution and image processing. Using digital imaging our approach faces these problems too. On the mathematical side, however, we replace the solution of the Laplace equation and the fitting process by a simple force balance applied to a cap of a droplet. Thus the equation for the surface tension becomes explicit. As we will see the key requirement of this method is a high grade pressure measurement. The difficulties with the Bond number as addressed in Ref. [3], which seem to exclude the oil/water case, do not materialize in our method.

One initial motivation of this work was the lack of interfacial tension data for the silicone oil/water system. References are sparse. A few data were found in references as quoted further down. In this work we use Wacker Silicone Fluid AK20 which is a poly dimethyl siloxane (PDMS) with an equivalent viscosity of 20 cS. This non-toxic, transparent fluid is widely used in chemical industry, food processes and so on.

The paper deals with the following topics. In chapter 2 we start with the analysis of the force balance leading to the equation for the interfacial tension. Chapter 3 explains the experimental set-up and evaluation procedure. Finally the results for the silicone oil/water system are presented along with an error analysis in chapter 4.

2. Principle of measurement

The principal arrangement is shown in Fig. 1. An oil drop attaches to a nozzle submerged in water. The nozzle forms the left leg of an oil-filled U-tube. At the bubble top, where $y = 0$, the water depth is h. In the right leg the oil pushes against an air cushion of pressure p_{air} which is somewhat larger than atmospheric, the difference being denoted $\Delta p_m = p_{air} - p_{atm}$. The interface shapes a meniscus at the distance h^* beneath the water line.

The basic idea is to exploit the vertical force balance on the cut-off cap shown in Fig. 2. At the cut-off plane the bubble cap has the width W and the height H. In vertical direction we identify the following force components.

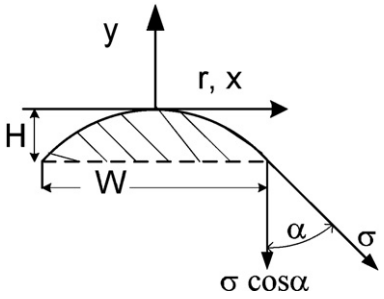

Fig. 2. Coordinates at the bubble cap.

The water pressure (density ρ_{ex}) on the cap contributes the downward force

$$-2\pi p_{atm}\frac{w^2}{8} - 2\pi g\int_0^{w/2}(\rho_{ex}(h - y(r)))rdr \quad (1)$$

where $y(r)$ means the contour function. Note that values of y are negative.

The interfacial tension σ pulls at the circumferential line in tangential direction of which the vertical part amounts to

$$-\pi W\sigma\cos\alpha \quad (2)$$

The third downward force is the gravity onto the oil in the cap. With the gravity acceleration g and the oil density ρ_{in} one gets

$$-2\pi\rho_{in}g\int_0^{w/2}(H + y(r))rdr \quad (3)$$

There is just one upward force due to the pressure acting at the cut-off plane

$$(p_{atm} + \Delta p_m - \rho_{in}g(h^* - H - h))\frac{w^2\pi}{4} \quad (4)$$

Balancing these four contributions leads finally to:

$$\sigma = \frac{g\rho_{ex}hW}{4\cos\alpha}\left\{\frac{\Delta p_m}{g\rho_{ex}h} + \frac{\rho_{in}}{\rho_{ex}}\left(1 - \frac{h^*}{h}\right) - 1 + \frac{8}{hW^2}\left[1 - \frac{\rho_{in}}{\rho_{ex}}\right]\int_0^{w/2} y(r)rdr\right\} \quad (5)$$

The right side of this equation lists the quantities which need to be known or measured.

3. Experimental arrangement

3.1. Mechanical design

The measuring cell (Fig. 3) consists of a cylindrical housing (71 mm i.d.) made from stainless steel. Both end faces carry windows spaced at 59 mm. The right leg of a U-tube runs vertically along the centre with a tight feed through at the bottom. It consists of very thin glass (5/10 mm) to minimize optical distortion. At the external bottom end it connects to a syringe which supplies oil to the U-tube (Silicone oil AK20 equivalent to 20 cS). The upper end branches to a pressure transducer (MKS-Baratron 698A11TRB, 10 Torr range), a vent and a volume displacing bellows sensitively operated by a fine spindle. The other leg serves as the bubble producing nozzle. It is made from brass tubing with 1 mm internal and 1.5 mm external diameter. For vibration damping, cell and auxiliary equipment are mounted on a heavy granite table as used for delicate optical set-ups (Fig. 4).

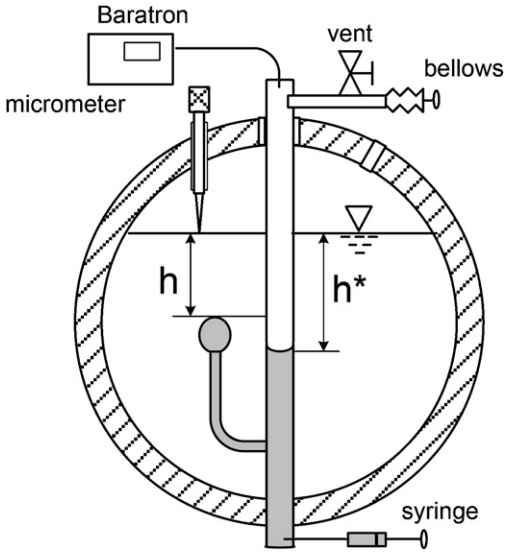

Fig. 3. Cross sectional view of the measuring cell.

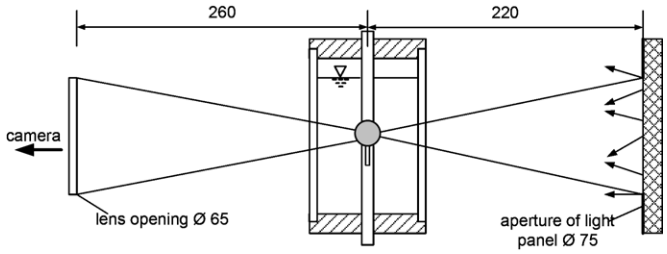

Fig. 4. Optical set-up. Measures in mm.

The bubble making starts with oil filled up to the nozzle exit while the vent is open. Then the vent is closed and water is filled in. Now the bellows is actuated to increase the air pressure p_{air}. The rising pressure pushes the oil down and the bubble emerges at the nozzle at a proper size. When the bubble has been made the pressure difference Δp_m is recorded and an image is taken (Fig. 5).

For the evaluation of σ the heights h and h^* are needed. They can be read pixelwise from the image supposing the water line is properly visualized (it appears blurred due to the meniscus forming at the windows). Visualization is achieved by a needle tip lowered to the water line by a micrometre at the centre of the cell. When the tip contacts the water it creates a black dot which is perfectly visible.

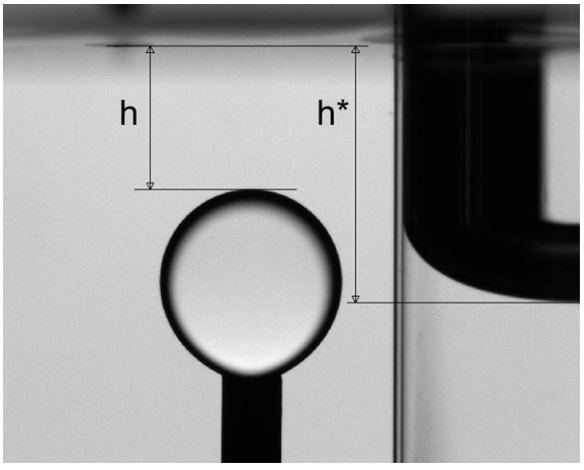

Fig. 5. Image of the bubble, the oil meniscus in the right leg glass tube and the needle point touching the water line.

The following optical set-up shows how the image is taken.

3.2. Optical set-up

Illumination is realized by a light panel emitting diffuse white light. Its outlet is restricted by a circular aperture of 75 mm. The aperture and the distance from the bubble determine a half cone illumination angle of 7°. The refraction law demands that any ray hitting the oil ($n = 1.4$) from the water side ($n = 1.33$) is refracted into the bubble. According to Fresnel's law of reflection [8] the reflected portion of the light increases exponentially with the angle of incidence, i.e. towards the bubble edge. This means that the bubble rim receives increasingly less light than the centre. Therefore the bubble centre appears bright while the bubble rim stays dark.

At the same time this means that the bubble edge is imaged by those rays which merely touch the edge. These are rays from a narrow angular range of 7°. They are received by the lens (Zeiss Macro Planar T*2,8/100) focused on the perimeter in the bubble centre plane. The image of the edge forms on the chip of a CCD-camera (Imager Pro X4M). It features 14 bit grey resolution with 2048 × 2048 pixel. The magnification is adapted to the size of the chip (15 mm × 15 mm) to get good resolution.

The entire set-up is housed in an insulated box which can be cooled to 15 °C or heated to 35 °C.

3.3. Evaluation of σ

For the evaluation of σ the right side of Eq. (5) has to be provided. For g we take 9.81 m/s^2. The water density ρ_{ex} as function of temperature is taken from Ref. [9] and the oil density ρ_{in} from Ref. [10]. The pressure Δp_m is measured as mentioned. It is of the order 80 Pa. It is corrected by taking into account the meniscus in the glass tube. The meniscus is evaluated in analogy to the cap evaluation. The correction amounts to 3.3 Pa.

The contour function $y(r)$ of the cap entering the integral is determined by image processing [11].

The 2-D pixel image taken by the CCD-camera is grabbed and stored by the software package DaVis 7.2 by LaVision in the "imx" format for post processing. It is then transferred to MATLAB using the function "loadvec". The contour finding is done by application of the tools "edge" and "bwtraceboundary" on the 2-D field of grey values. These tools identify gradients of grey values at any point in the field. When the gradients are large enough to overcome a preset threshold the point is identified as a contour element. A line of neighbouring contour elements make up the contour. In principle, this is a mathematical procedure and there is no unique mapping for the location of the contour in optical terms. Yet, the transition from dark to bright is only 4–8 pixels wide.

The identified contour points make up a curve $y(r)$. Along this curve the image is discretized into black (bubble) and white (water). Fig. 6 shows a section of the contour with the white line delineating bubble and water. Being evaluated from a pixel image the contour consists of discrete elements which we use directly for the numerical integration in Eq. (5). This simple and effective method becomes equivocal towards the meridian where y changes rapidly from one pixel to the next. To avoid this problem we stop the integration at $\alpha = 45°$. Here y and r change at the same rate.

The width W and the heights h and h^* are determined by pixel counting. Calibration of the length scale is accomplished by moving the needle tip of the micrometre in vertical direction for a known distance and recording the displacement by pixel-counting.

The whole evaluation relies on symmetry with respect to the drop axis. Due to disturbances at the nozzle mouth they sometimes are not quite symmetric. To warrant symmetry one branch

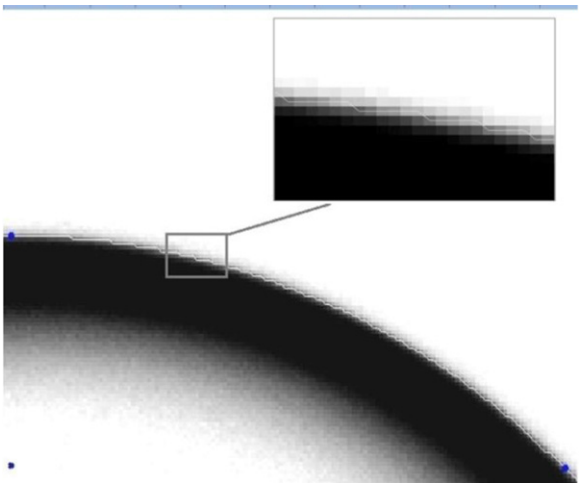

Fig. 6. Enlarged section of the bubble contour with the white contour line from image processing.

of the evaluated contour is rotated about the vertical axis and compared with the opposite branch. The radial distance between the curves is related to the radius itself. When this ratio exceeds 0.5% the evaluation is discarded.

4. Results

Fig. 7 displays the results for the oil/water system together with the data for pure water and for pure oil in the temperature range 18–35 °C. For σ of water we refer to Ref. [9] and for oil to Ref. [10]. The two liquids affect each other considerably in producing an intermediate interfacial tension notably remote from the individual values. A physically accountable estimate [1] is the square root of the product of both tensions with a pre-factor of one which comes to about 38 mN.

Scattered data points for comparison are sparse and found in various contexts where silicone oil was used with water. A rather old source is [4] where among other oil properties a value of 40 mN/m is quoted. A work on rotating oil/water stratifications [6] uses 28 mN/m which seems doubtful since they measure 49.14 mN/m for water which is far off the book value. A recent paper on the new method of electro-wetting claims 38 mN/m for calibration purposes [7]. Yet, their water has traces of salt in it. The actual results of an up to date ring measurement were communicated to

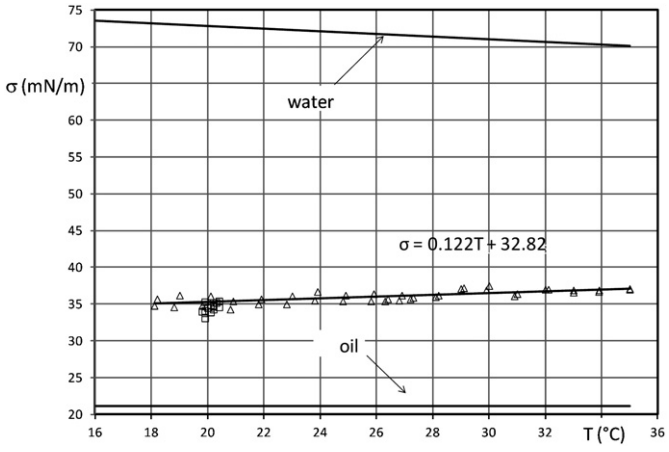

Fig. 7. Results for the interfacial tension between silicone oil (20 cS) and water.

me by A. Juel [5]. They agree very well with our result, however they were taken for higher viscosities (34.4 mN/m for 1000 cS and 35.1 mN/m for 12500 cS at 25 °C).

For data representation a linear curve fit is inserted in the diagram. It shows a weak increase with temperature. A close look reveals pairs of points. Those were taken right after temperature and bubble were established and ten minutes later. No distinguished altering beyond that pair forming could be observed.

The max/min scatter about the linear fit is ±1.1 mN/m at an rms value of 0.53.

To be sure that the scatter about the linear fit is representative ten experimental runs at 20 °C were repeated with the whole procedure from image taking to evaluation. The results appear as a cluster of points at 20 °C in agreement with the scatter about the linear fit in the entire range.

The source of the scatter among repeated experiments is explainable by the measuring accuracy of the involved quantities. This can readily be estimated due to the explicit character of Eq. (5) which allows to write the partial derivatives with respect to the measured quantities h, h^*, Δp_m, and W

$$\frac{\partial\sigma}{\partial h} = \frac{g\rho_{ex}W}{4\cos\alpha}\left\{\frac{\rho_{in}}{\rho_{ex}} - 1\right\} \tag{6}$$

$$\frac{\partial\sigma}{\partial h^*} = -\frac{g\rho_{in}W}{4\cos\alpha} \tag{7}$$

$$\frac{\partial\sigma}{\partial\Delta p_m} = \frac{W}{4\cos\alpha} \tag{8}$$

$$\frac{\partial\sigma}{\partial W} = \frac{g\rho_{ex}h}{4\cos\alpha}\left\{\frac{\Delta p_m}{g\rho_{ex}h} - 1 + \frac{W}{2h}\left[1 - \frac{\rho_{in}}{\rho_{ex}}\right]\right\} \tag{9}$$

Eq. (9) includes the (for this purpose) reasonable assumptions that the integral represents a spherical segment, cut at 45° and that h and h^* are of the same order. Using typical values for the measured quantities the derivatives can be calculated. Then they are multiplied by the measurement tolerances. For the length we used $\pm 20 \times 10^{-6}$ m which is the equivalent of three pixels. For Δp_m, ±0.5 Pa is a reasonable setting for the following reason. The transducer has an accuracy of 0.05% of reading. For a typical value of 80 Pa that would amount to only ±0.04 Pa. However, due to vibrations of the building reaching the drop despite the granite table or other unknown influences the reading fluctuates for about ±0.3 Pa. Therefore, ±0.5 Pa is a conservative estimate.

With these settings we find deviations of σ with respect to the length scales of clearly less than 1 mN/m. The critical parameter is the pressure. The calculated deviation reaches the order of ±1 mN/m. Looking at the results the max/min scatter about the trend line amounts also to ±1 mN/m. Therefore, it can be said that the method depends primarily on the pressure measurement. A high grade pressure transducer like the used Baratron is indispensable.

5. Conclusion

In this work drop contour data are used to determine the interfacial tension between liquids without involving the Laplace equation. The basis is a force balance applied to a bubble cap which provides an explicit equation for σ. The measured quantities entering this equation are lengths measured pixel-wise and a pressure. It turns out that the pressure measurement is crucial for the accuracy.

The method is demonstrated for an oil drop in water in the temperature range 18–35 °C. A slight linear temperature trend appears. The scatter of the data about the linear fit corresponds reasonably with the attainable accuracy. The determined interfacial tension lies somewhat closer to that of oil than to that of water which means

that the molecular orientation of the water molecules in a free surface is strongly affected by oil molecules although they are perfectly hydrophobic.

Considering the bleak data situation for the oil/water case with enormous scattering between the few available sources we think that our method has considerable potential.

References

[1] A.W. Adamson, A.P. Gast, Physical Chemistry of Surfaces, Wiley, New York, 1997.
[2] S. Lahooti, O.I. Del Rio, A.W. Neumann, P. Cheng, Axisymmetric drop shape analysis (ADSA), in: A.W. Neumann (Ed.), Applied Surface Thermodynamics, Dekker, New York, 1996.
[3] N.J. Alvarez, L.M. Walker, S.L. Anna, A non-gradient based algorithm for the determination of surface tension from a pendant drop: application to low Bond number drop shapes, J. Colloid Interface Sci. 333 (2009) 557–562.
[4] H.W. Fox, P.W. Taylor, W.A. Zisman, Polyorganosiloxane surface active properties, Ind. Eng. Chem. 39 (11) (1947) 1401–1409.
[5] A. Juel, University of Manchester UK, Personal communication.
[6] A.S. Berman, J. Bradford, T.S. Lundgren, Two-fluid spin-up in a centrifuge, J. Fluid Mech. 84 (3) (1978) 411–431.
[7] A.G. Banpurkar, K.P. Nichols, F. Mugele, Electrowetting-based microdrop tensiometer, Langmuir 24 (2008) 10549–10551.
[8] E. Hecht, Optics, 4th ed., Addison-Wesley, Reading, MA, 2002.
[9] W. Wagner, A. Kruse, Properties of Water and Steam: The Industrial Standard IAPWS IF97, Springer, Berlin, 1998.
[10] A.C.M. Kuo, Poly(dimethylsiloxane), in: Polymer Data Handbook, Oxford University Press, New York, 1999, pp. 411.
[11] R.C. Gonzales, R.E. Woods, S.L. Eddins, Digital Image Processing, Pearson Prentice Hall, New Jersey, 2004.